Scientific Research Publishing

American Journal of Analytical Chemistry, 2022, 13, 255-276
https://www.scirp.org/journal/ajac
ISSN Online: 2156-8278
ISSN Print: 2156-8251

Microwave-Assisted Inactivation of Fomite-Microorganism Systems: Energy Phase-Space Projection

Victor J. Law*, Denis P. Dowling

School of Mechanical and Materials Engineering, University College Dublin, Dublin, Ireland
Email: *viclaw66@gmail.com

How to cite this paper: Law, V.J. and Dowling, D.P. (2022) Microwave-Assisted Inactivation of Fomite-Microorganism Systems: Energy Phase-Space Projection. *American Journal of Analytical Chemistry*, **13**, 255-276.
https://doi.org/10.4236/ajac.2022.137018

Received: June 28, 2022
Accepted: July 25, 2022
Published: July 28, 2022

Abstract

This paper describes the use of log-linear energy phase-space projections to analyze microwave-assisted inactivation of bacteria and viruses under different fomite conditions within multimode microwave ovens. The ovens are operated at a cavity-magnetron frequency of 2.45 ± 01 GHz. Porous fomites (moist face towels, cotton swabs, kitchen sponges, and scrubbing pads, cigarette filters and N95-like respirators); along with non-porous hard surface syringe fomites are studied. The fomites are classed as dielectric; and absorb microwave energy to varying degrees depending on their complex dielectric permittivity. Microorganism resilience to microwave stress (defined as ≥4 $\log_{10}$ reduction in inactivation) when mapped using iso-volume trend-lines in energy phase-space reveals the persistence imparted by the fomite, and can be mapped between different microwave ovens. Microorganism resilience to thermal microwave-assisted treatment increases from vegetative Gram-negative to vegetative Gram-positive and on to Gram-positive spores. Bacteriophage MS2 and influenza viruses have an intermediate resilience dependency. It is shown that linear-scaled fomite temperature against process time graphs can differentiate between non-thermal and thermal microwave-assisted treatment of microorganisms.

Keywords

Bacteria, MS2, Hepatitis C Virus, Human Immunodeficiency Virus, Influenza Virus, Disruption, Inactivation, Microwave Oven, Data Analysis

1. Introduction

Some of the earliest reports of domestic multi-mode microwave oven use as an energy source (100 Ws at 2.45 ± 0.01 GHz) for microwave-assisted extraction

(MAE) of organic compounds may be found in [1] [2] [3] [4] [5]. Of particular note is the description of rapid microwave induced bacteria and virus lysis as compared to chemical, thermal, and ultrasonic lysis [2] and autoclave [3]. In this work the term microwave-assisted, rather than microwave-shock is used. Pulse and discontinuous electric fields stress (6 to 7 kV) in the GHz frequency range have been used to study non-thermal microwave-assisted disruption and inactivation of vegetative bacteria and bacteria spores [6] [7] [8], but their comparative cost compared to the domestic microwave oven may be prohibitive in a laboratory and day to day home environment. From a microorganism point of view, the logical outcome of lysis is cell death, which has become an important subject of research since the impact of human immune deficiency virus (HIV) and more lately the SARS-CoV-2 pandemic [9] [10]. For example, using batch microwave oven treatment of hepatitis C virus (HCV) and HIV-1 [11], and bacteria [12]-[18] can produce a $\geq 4\log_{10}$ reduction in inactivation. Furthermore, continuous flow microwave oven irradiation has produced similar reductions in bacteria [19] [20] and Virus inactivation [21]. Batch microwave generated stream (MGS) decontamination (within a multi-mode microwave oven) of influenza virus inculcated N95-like respirators have been reported [22]-[27].

The complex area of microwave-assisted cell injury, disruption, and inactivation span a broad spectrum of scientific disciplines from biology, virology, and thermodynamics to radio engineering. In 2021, we reviewed the thermodynamics and dielectric conditions required for batch MGS decontamination of N95-like respirators within multi-mode microwave ovens [28] [29]. In the following year, the microwave multi-mode microwave oven detection, disruption, and inactivation of bacteria and virus within fluid culture suspension and different imamate surfaces (fomites) were reviewed [30]. This work extends the thermodynamic analysis within [19] [28] [30] by extending the use of phase-state projections to map bacteria and virus microwave-assisted inactivation in: liquid suspension, suspension filled porous fomites and suspensions on non-porous hard fomite surfaces. It is noted, that in all of these treatments water moisture content is present, which enhances the inactivation process as compared to dry-heat treatment [22]-[29]. This new mapping process provides a means of comparing historical microwave-assisted inactivation data thereby allowing researchers to extend boundaries of understanding the effects of both thermal and non-thermal microwave-assisted inactivation.

The construction of the energy phase-state projection requires the conversion of three quantities (process energy budget, energy density, and inactivation reduction) into a 2 dimensional representation of the microwave-assisted treatment. In this projection, the process energy budget and energy density are held true on either the horizontal and vertical axis, while inactivation reduction is compressed to $\geq 4\ \log_{10}$. The $\geq 4\ \log_{10}$ value is based on the initial inactivation valve from each reference paper, and is calculated either as a Log_{10} reduction ($\text{Log}_{10}(A/B)$), or percentage reduction ($A - B * 100/A$) as a function of experiment conditions. As in all datasets however the collected data from different re-

search sources, the experimental conditions (chemical and instrument sensitivity) are not reported in a consistence manner [28]. For example, for reviewing thermal inactivation of coronavirus strains, Abraham *et al.* 2020 [31] used a 7 $\log_{10}$ reduction to account for a total reported inactivation. Here, an inactivation reduction of ≥4 $\log_{10}$ is used as a measure of resilience [32] [33] before the fomite-microorganism system moves into a different region of state space when subjected thermal heat, or microwave-assisted stress.

Figure 1 presents a re-drawing of the original ≥ 4 $\log_{10}$ inactivation energy phase-space projections of Gram-negative, Gram-positive and virus suspension in open beaker [12] [14], kitchen soaked sponge [16], plus kitchen soaked scrubbing pad [16]. The process energy budget (kJ) on the horizontal-axis against the specific energy density (kJ·ml^{-1}) of the suspension on the vertical-axis. A least square trend-line ($y = 0.015x$, intercept = 0.0, $R^2 = 0.9854$) fitted to the combined open beaker and kitchen soaked sponge datasets. This mapping process reveals the Gram-negative vegetative *E. coli* is the most susceptible to microwave irradiation and the Gram-positive *B. cereus* spores are the most resilient. In between these extremes the vegetative *B. cereus* and the MS2 virus are presents. The kitchen soaked scrubbing pad outlier dataset pad [16] is an example of how fomite appears to influence the inactivation resilience of *E. coli*.

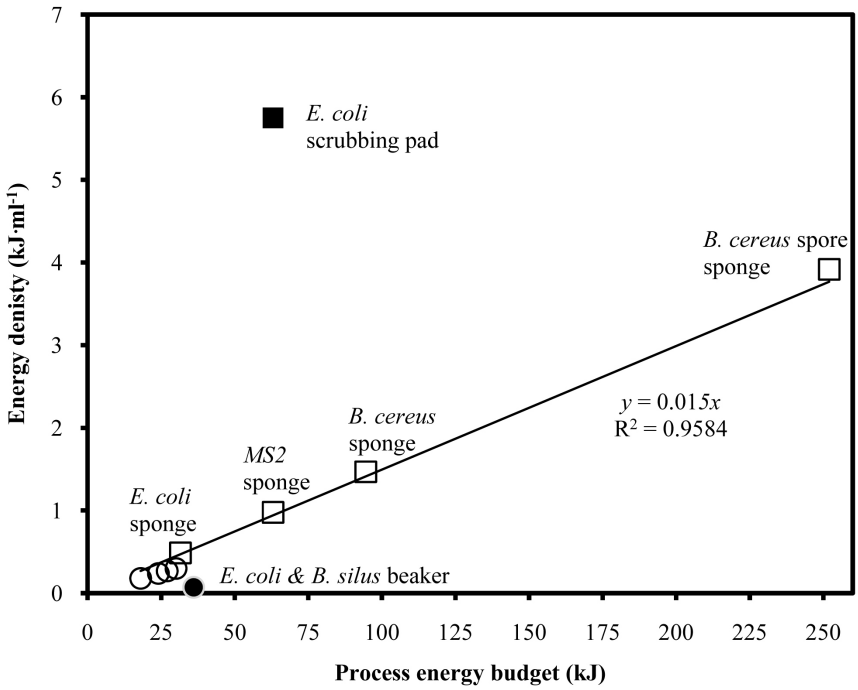

Figure 1. Energy phase-space projection of microwave-assisted bacteria and virus ≥ 4 $\log_{10}$ inactivation. *Escherichia coli* (*E. coli*) 100 ml suspension within open beaker; open circles (100 to 300 W [12]). *E. coli* and *B. subtitles* in 500 ml suspension beaker; black circles (600 W [14]). *E. coli*, MS2, *B. cereus* and *B. cereus spores* kitchen soaked sponge; open squares (1.05 ± 0.050 kW [16]). *E. coli*, kitchen scrubbing pad; black squares (1.05 ± 0.050 kW [16]). In each case, the suspension temperature is recorded to be in the 70 to 90˚C range.

The aim of this work is to analysis the deterministic variables involved in multi-mode domestic microwave oven inactivation of bacteria and virus. The analysis uses energy phases-space projections to map the microwave-assisted process in 2-dimensional where the coordinate enable a clear differentiation between the porous fomite (moist face towels, cotton swabs, kitchen sponges and scrubbing pads and N95-like respirators) and the bacteria or virus suspension contaminate on hard surface fomite (syringe). All of the fomites studied here, have baulk dielectric properties, which are altered by the suspension fluid and therefore influence the amount of the microwave energy absorbed in the suspension during its heating. One way to calculate the binary mixture effective dielectric constant is to use a modified Looyenga cubic mixing formula [34]. Metal fomites, such as scalpel blades [35] that reflect microwave energy [30] [36] are not studied here. To achieve the stated objective, this paper is constructed as follows. Section 2 looks microwave oven power calibration. Section 3 provides a baseline description of vegetative spore bacteria, non-enveloped and enveloped virus structural arrangement that are contained within the analysis. To aid the understanding of microwave-assisted inactivation, post treated surface morphology and cytoplasm damage is given using published: optical microscope, scanning electron microscope (SEM) and transmission electron microscope (TEM) images. Section 4 lists the microwave oven fomite-microorganism inactivation experiments examined in this work. With the knowledge assembled in Sections 2 to 4, Section 5 develops the interpretation of energy phase-state projections. Section 6 considered non-thermal and thermal microwave-assisted projections. Section 7 provides a summary and outlook.

2. Microwave Oven Power Calibration

The microwave ovens employ a free-running cavity-magnetron operating a frequency of f_0 = 2.45 ± 0.05 GHz as the energy source. Normally the cavity-magnetron manufactures stated power, is calibrated using the open water bath method, where the temperature rise of water (1000 ml) is measured over time for a given power level setting [28] [29] [30] [37] [38] [39] [40] is based on Equation (1).

$$P = mC\frac{\Delta T}{t} \tag{1}$$

where P is power (W, or J·s^{-1}), m is the mass (g) of water, C is heat capacity (4.184 J·g^{-1}·K^{-1}) of water, ΔT is the change in water temperature (final temperature minus the initial temperature), and t is the heating time measured in seconds. Given this method of power calibration for a domestic microwave oven, at full power the cavity-magnetron operates in the continuous wave (CW) mode, or duty-cycle (D) = 100%. For values of $D \geq 100\%$, the cavity-magnetron is sequentially pulsing on and off the cavity-magnetron. For example, a power setting that employs D = 50%, the on-period (t_{on}) is equal to the off-period (t_{off}). Whether or not CW is used, this aspect of microwave irradiation is generally

termed "thermal" microwave-assisted dielectric volume heating (**Figure 2(a)**). When attempting to achieve sublethal conditions for microwave-assisted injury or disruption of microorganisms, the suspension is generally surrounded with an ice/water vessel to cool and control the temperature of the suspension that is being irradiated. This process has been called "athermal" [15] (or, "non-thermal" [17]) microwave-assisted heating, where typical suspension temperatures of 20˚C to 29˚C are obtained (**Figure 2(b)**) using microwave power applied from the oven's cavity-magnetron, operating in the non CW mode [15] [17]. For values of $D > 100\%$, the "athermal" and "non-thermal" terms become ambiguous due to the addition of time modulated of applied microwave energy, making the attempt to separation out thermal heating effect from the microwave irradiation effects complex. For microorganisms however, when looked at in detail for a given applied microwave power source, the ice/water vessel acts as a dumpy-load by absorbing microwave energy via the process of dielectric volume heating [36]-[46]. Secondly, the dummy load extracts heat from the outer surface of the suspension vessel. The first of these two contrasting heat loss pathways changes the water solid-phase (ice) into water liquid-phase where the latent heat of fusion of the ice is 336 $J \cdot g^{-1}$ @ 0˚C. This is followed by heating of the water liquid-phase volume from 0˚C to the final temperature reached at the end of the microwave heating period. The conduction heat loss pathway may be considered to be localized, independent of molecule polarity, and proceeds at a slower rate than the rapid heat change involved in dielectric volume heating. The overall effect is to divert a portion of the cavity-magnetron power that who have otherwise been applied to the suspension volume. In this context, whether the ice/water dummy-load provides a non-thermal dimension to the microwave-assisted heating of microorganism is examined further in Section 6.

Outside the realm of microwave-assisted microorganism injury, disruption and inactivation, compressed air forced cooling is used in organic synthesis to maintain a particular temperature with simultaneous microwave irradiation to produce a particular transition state in order to increase the yield of a target compound that would not have be obtained by thermal heating alone [4] [41]

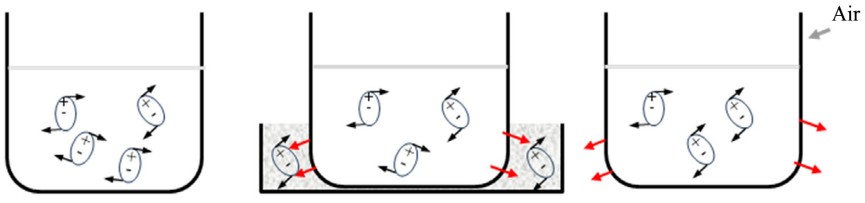

Figure 2. (a) Thermal microwave-assisted. (b) Ice/water bath non-thermal microwave-assisted [15] [17]. (c) Air forced microwave-assisted treatment [4] [41] [42]. Red arrows indicate the direction of heat loss from the system; rotating positive and negative symbols indicate regions of dielectric volume heating.

[42] [45] [46]. **Figure 2(c)** shows the general direction of air cooling under microwave irradiation conditions, and the forced heat transfer from the microwave heated vessel and its suspension.

3. Inactivation Mechanism of Bacteria and Virus

In many cases, the role the microorganism membrane is to provide a rigid and elastic boundary that determines the bacteria cell shape (rod, or spherical) and to protect the cell cytoplasm from a changing physical and chemical external environment. For example, it is generally considered that thermal heat inactivation (denaturation) of microbial homogeneous populations follow a first-rate law [12] [43] and mixed populations follow a non-first-order-rate law [43]. Mathematically, first-order-rate kinetics may be expressed as in equation (2).

$$[C] = [C_o] e^{-kt} \tag{2}$$

where $[C]$ is the reduction in living microorganism concentration, $[C_o]$ is the initial living microorganism concentration, k is the rate constant, and t is time.

In this work, experimental studies of microwave-assisted inactivation of homogeneous populations of bacteria and virus are examined. In these studies the microwave electric field energy couples in to the biological material (lipids, proteins, carbohydrates, DNA, and water) with varying degrees of efficiency. As the electromagnetic waves penetrate the biological entity, their dipolar molecules are vibrated causing dielectric volume heating. To help understand the resilience of microorganisms to microwave irradiation, this section is divided into the following sections; Gram-negative and Gram-positive bacteria (Section 3.1), non-enveloped (Section 3.2), and enveloped virus (Section 3.3).

3.1. Gram-Negative and Gram-Negative Bacteria

Hans Christian Gram (1853 to 1938) helped to developed specific dyes to differentiate microorganisms when viewed under a microscope. Today the term Gram-negative and Gram-positive (**Table 1**) is used to differentiate between bacteria that have one or two semi-permeable membranes.

Bacteria Lysis and Membrane Rupture

Figure 3 shows a simple mechanical membrane structure for both gram-negative and gram-positive bacteria [47]-[52]. In the case of Gram-negative bacteria (**Figure 3(a)** and **Table 2**), they have an outer membrane that provides a barrier to the outside environment, and controls the regulation of osmotic pressure within the periplasmic space that is bounded by the cytoplasm membrane and outside layer of the outer membrane that faces the outside environment. The peptidoglycan (~4 nm thick) consists of disaccharide repeating units that have two contrasting functions: to act as a semipermeable macro-molecular cellular exoskeleton to the cytoplasm membrane, and to withstand the cytoplasm turgor pressure. In addition, lipopolysacchaides, and lipoproteins that are anchored to the inside of the outer membrane add both additional structural support to the

outer membrane and provide a hydrophilic outer surface that helps osmotic regulation. For example, a decrease in external osmotic pressure causes water influx and cell swelling, and if uncontrolled, lysis occurs followed by membrane rupture and cell inactivation and ultimately to cell death. In the opposite sense, an increase in external osmotic pressure causes water extraction, dehydration and in the extreme case triggering spore formation.

Table 1. Gram-negative and gram-positive vegetative bacteria reported to undergo multi-mode microwave oven-assisted membrane rupture.

Microorganism	Single cell shape	Typical volume	Reference
	Gram-negative		
M. aeruginosa	Rod-shape: 4 to 5 mm in length and 1 to 1.5 μm diameter (biofilms)	7 mm^3	[1]
E. coli	Rod-shape: 2 to 6 μm in length and 1 to 1.5 μm diameter	6 mm^3	[4] [12] [14] [15] [16] [17] [20]
P. aeruginosa	Rod-shape: 1 to 5 μm long and 0.5 to 1 μm diameter	1 mm^3	[13]
P. fluorescens	Rod-shape: 1 to 5 μm long and 0.5 to 1 μm diameter	1 mm^3	[19]
	Gram-positive		
B. cereus	Rod-shape: 3 to 4 μm in length and 0.25 to 1 μm diameter	2 mm^3	[16] [18]
B. subtilis	Rod-shape: 4 to 10 μm in length and 0.25 to 1 μm diameter	3 mm^3	[14]
B. subtilis var niger spore (airborne)	Rod-shape: 4 to 10 μm in length and 0.25 to 1 μm diameter	3 mm^3	[19]
S. aureus	Spherical-shape: 0.5 to 1.5 mm in diameter	2 mm^3	[13] [27]

Table 2. Reported optical microscope, SEM, and TEM imaging of bacteria inactivated by microwave-assisted treatment morphology and cytoplasm electron-density.

Microorganism	Optical microscope	SEM	TEM	Ref
Gram-negative				
E. coli suspension		Morphological disruption	High and low electron-dense cytoplasm	[14]
E. coli suspension	Differential fluorescent staining: disruption off membrane			[15]
P. fluorescens airborne		Morphological change	High and low electron-dense cytoplasm	[19]
Gram-positive				
B. subtilis suspension		No change	High and low electron-dense cytoplasm	[14]
B. subtilis airborne		Morphological change	High and low electron-dense cytoplasm	[19]
A. versicolor airborne		Morphological change	High and low electron-dense cytoplasm	[19]
B. cereus suspension		Morphological disruption	High and low electron-dense cytoplasm	[18]

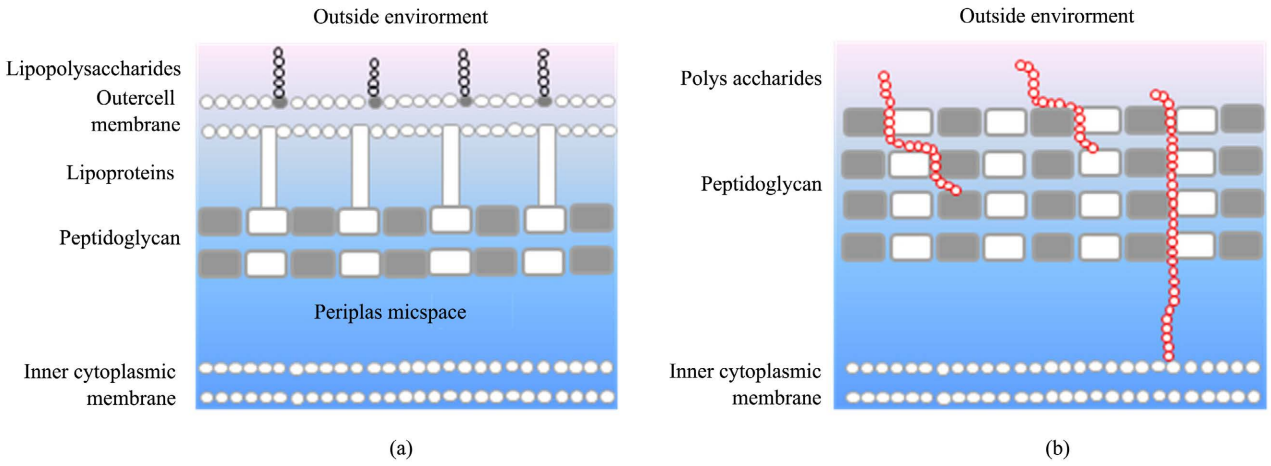

Figure 3. (a) Gram-negative bacteria cell wall: *Microcystis aeruginosa* (*M. aeruginosa*), *E. coli*, *Pseudomonas aeruginosa* (*P. aeruginosa*), *Pseudomonas fluorescens* (*P. fluorescens*) have an inner bilayer cytoplasm membrane surrounded by a thin rigid, elastic, and semipermeable wall (peptidoglycan) that is bounded by an outer lipid bilayer membrane. (b) Gram-positive bacteria cell wall (*Bacillus subtilis var niger* (*B. subtilis var niger*) and *Staphylococcus aureus* (*S. aureus*) have a similar inner bilayer cytoplasm membrane surrounded by a thicker peptidoglycan.

Gram-positive bacteria do not have an outer membrane or lipoproteins, but have an extended, or thicker (~9 to 33 nm), peptidoglycan which quickly becomes stained in the Gram stain test. Without an outer membrane by definition there is no periplasmic space. These bacteria also contain polysaccharides that are covalently attached to the peptidoglycan (**Figure 3(b)** and **Table 2**). Today it is thought the extended peptidoglycan can withstand greater cytoplasm turgor pressures with respect to Gram-negative bacteria and therefore Gram-positive bacteria have a greater resilience to outside osmotic pressures.

Manmade induced osmotic pressure imbalance and hence triggering cell lysis may be performed using a mechanical, chemical, thermal, electrical, ultrasonic, autoclave or microwave method [1] [2] [3] [4] [5] and in the extreme case by explosive decompression [53] [54]. In each of case, the purpose is to extract cytoplasm material (deoxyribonucleic acid (DNA) or ribonucleic acid (RNA)) material for further use. In this context, the purpose of microwave-assisted inactivation may be considered to be complete after microwave treatment.

3.2. Non-Enveloped Virus Structure

Bacteriophage MS2 virus has an icosahedral (60 rotational symmetries) capsid with a typical average near-spherical diameter of 25 to 28 nm, making it one of the smallest known viruses. Tightly packed within the capsid is a positive-sense single-stranded RNA. Pores within the capsid wall allow water and ion transport across the wall. Even though MS2 has no outer envelope it is communally used as a surrogate for influence virus in aerosol studies [21] and MGS decontamination of inoculated N95-like respirator studies [22] [24] [26]. Due to their nanoscale, SEM, and TEM imaging is unable to resolve microwave-induced changes in morphology and internal damage.

Wu *et al.* [21] used a modified microwave oven (Midea Inc., Foshan, Guangdong Province, China) to inactivate airborne MS2. Three microwave power settings where used (119, 385 and 700 W). At the highest power 700 W and 2 minutes irradiation an inactivation of approximately 90% was achieved as determined by *E. coli* host qualification.

3.3. Enveloped Virus Structure

H1N1 and H5N1 influenza virus [23] [25], HCV and HIV-1 [11] are classed as enveloped virus that have icosahedral symmetries with a size one tenth the size of bacteria (typically 40 to 150 nm in diameter and 1.7×10^6 nm^3 in volume). Within the envelope is the capsid that contains a positive-sense single-stranded RNA. The outer envelope is formed by a lipid double layer derived from modified host cell material, along with embedded glycoprotein spikes that give the virus its distinctive appearance. When traveling outside an infective body and through environmental temperatures these viruses have an infection persistence of a few hours to ten days depending on the fomite that is carrying it. With increasing temperature (above of 30˚C) the duration of persistence becomes shorter. Here again SEM and TEM are unable to resolve changes in morphology and internal damage.

4. Fomites

Due to the varying infection persistence of microorganism on, or within, different fomites [55] it is important to analysis the amount of microorganism suspension fluid within different soft and porous fomites, and hard non-porous surfaces of filled syringes and empty syringes. This section lists the salient energy details of moist face towels, cotton swabs, kitchen sponge, and scrubbing pad, syringes, and cigarette filters are listed below. Microwave generated steam decontamination of N95-like respirator studies are listed in a separate group at the end of this section. One of the aims of these studies was to kill the microorganisms whilst keeping the physical and visual properties of the fomites intact with a view to re-use.

Moist face towels

In 1998, Tanaka *et al.* [13] reported on microwave oven (Corona Co., Ltd., Tokyo) sterilization of moist face towels that where inoculated using (1 ml aliquots on 7 × 7 cm gauze) of *S. aureus*, *P. aeruginosa* and *C. albicans*. Were the goal of the study was to decontaminate used towels to a level that the towels were suitable for re-use in the care of aged persons and bedridden patients. In this study the procedure of microwave-assisted sterilization of inoculated towels required the soaked face towel to be wrung tightly and wrapped in warping film, and then microwave irradiated. However the size of neither the face towel nor the amount of remaining contaminated water within the towels is given. The towels were irradiated at a continuous wave (CW) power of 500 W for 60 seconds (30 kJ) for a single moist towel and 120 seconds (60 kJ) for three moist towels.

Cotton swabs

Elhafi *et al.* (2004) [3] used a domestic microwave oven (Sharp R-772(W)M) to decontaminate cotton swabs with wooden applicators that were dipped in Newcastle disease virus (NDV) or avian influenza virus (H1N1). The purpose of the study was to investigate whether microwave oven treatment would destroy the infectivity of NDV and H1N1 virus. Even though the authors do not give the amount of suspension absorbed on the swab, Zasada 2020 [56] indicates 0.05 to 0.15 ml of liquid is to be expected. Microwave oven irradiated at a CW power of 900 W for 20 seconds (18 kJ) was found to achieve total virus inactivation.

Kitchen sponges and kitchen scrubbing pads

Park *et al.* (2006) [16] studied microwave-assisted inactivation of *E. coli*, MS2, vegetative *B. cereus* and *B. cereus* spore inoculated kitchen sponge (3.17 × 3.37 × 0.69 cm: water capacity 64.3 ml), kitchen non-metallic kitchen scrubbing pad (9.06 × 7.07 × 0.65 cm: water capacity 10.9 ml). The material of the sponge foam and scouring pads were not given, but given related patent information at the time the martial used is most likely to be open-cell polyurethane foam and non-woven nylon, respectively [57]. A Sharp RE-S630D0 microwave oven was used as the microwave energy source (rated CW power of 1 or 1.1 kW; reported here as 1050 ± 0.050 W). The microwave inactivation time ranged between 30 and 240 seconds yielding a process energy budget of 31.5 to 252 kJ, with a measured fomite temperature between 80˚C to 92˚C.

Syringes and cigarette filter

Park *et al.* (2006) [16] reported on the inactivation of vegetative *E. coli*, bacteriophage MS2 and *B. cereus* spores from the inside surfaces of empted contaminated plastic 10 ml syringe. The aim of these experiments was to find a safe dispose method for contaminated syringes in a home environment. For these experiments a microwave oven (Sharp RE-S630D0, rated CW power of 1 or 1.1 kW (reported here as 1050 W). According to Cambruzzi and Macfarlane (2021) [58] remaining liquid within the syringe is of the order of 0.1 ml. A $\geq 4 \log_{10}$ inactivation was achieved at 420 seconds (441 kJ, 86.4˚C to 105.2˚C). Siddharta *et al.* 2016 [11] reported upon microwave oven (type: MM817ASM) inactivation of HCV and HIV-1 spiked 40 ml insulin syringes and cigarette filters with the aim to mimic re-use within a population of people who inject drugs (PWID). From the work of Register (2000) [59], it is reasonable to assume that the cigarette filter spiked volume is of the order of 0.5 ml. The syringe and cigarette filter were irradiated at a rated CW power 360 W for 180 seconds (180 kJ, ~70˚C) to achieve $\geq 4 \log_{10}$ inactivation.

N95-like respirators

The aim of these studies was to kill the microorganisms whilst keeping the physical and visual properties of the respirators intact with a view to re-use the respirators. For this dual requirement, the applied energy in the form of dielectric volume heating needs be to sufficient to kill the virus but not sufficient to damage the fomite. Thus the MGS defines an upper limit to the energy budget

similar to those sterilizing towels and cigarette filters. Below 70˚C it is found that there is insufficient: virus inactivation, whereas at the boiling point of water (100˚C) and prolonged irradiation times there is a loss of respirator filter void, loft, and structural failure at respirator component interface. The process window information of four studies is given below.

- Fisher *et al.* [24] used a Shape R-305KS microwave oven for MGS decontamination of MS2 inoculated N95-like respirators. The inoculated respirators where placed in a sterilizer bag which contained 60 ml of tap water as the steam source, then irradiated at a measured power of 750 W for 90 seconds (67.5 kJ) to achieve ≥4 $\log_{10}$ inactivation.
- Heimbuch *et al.* [23] and Lore *et al.* [25] both used a Panasonic Inverter microwave for MGS decontamination of H1N1 and H5N1 inoculated N95-like respirators, respectively. Heimbuach used 50 ml of tap water in two open water baths, and Lore used 50 ml of tap water as the steam source and a irradiation at a CW power 1250 W for of 120 seconds (150 kJ) to achieve ≥4 $\log_{10}$ inactivation.
- Zulauf *et al.* [26] used two unspecified microwave ovens that are rated at 1100 and 1150 W for MGS decontamination of MS2 inoculated N95-like respirators. In each case 60 ml of distilled water in an open water bath was used as the steam source and an irradiation at their respective CW power setting for 180 seconds (198 and 207 kJ) to achieve ≥5 $\log_{10}$ inactivation.
- Pascoe *et al.* [27] used a NE-1853MGS Panasonic microwave oven to decontaminative N95-like respirators that where inoculated with *S. aureus*. In this case 200 ml of deionized water within in a Tommy Tipee sterilizer was the steam then irradiated at rated CW power of 1800 W for 90 seconds (162 kJ) to achieve ≥4 $\log_{10}$ inactivation.

5. Interpretation of Energy Phase-State Projections

This section describes the mapping and interpretation of energy phase-state projections of microwave-assisted bacteria and virus inactivation on different fomites: moist face towel, cotton swabs, kitchen sponges and scrubbing pad, syringe and cigarette filters and N95-like respirators.

5.1. MGS Decontamination of N95-Like Respirators

This section overlays the MGS decontamination of N95-like respirators datasets onto the vegetative *E. coli*, MS2, vegetative *B. cereus*, and *B. cereus* spore inactivation trend-line. The trend-line is constructed from 10 datasets [12] [14] [16] with the slope property: $y = 0.015x$, intercept = 0.0, $R^2 = 0.9854$ as in **Figure 1**. The purpose of this overlay process to indentify similarities and dissimilarity between them. **Figure 4** shows the outcome of this comparison with the MGS data shown as open triangles with open water bath and sterilizer water purity annotated as tap water (T) deionized water (DI) and distilled water (Dis). In addition, the kitchen scrubbing pad [16] is given as reference point to aid the eye.

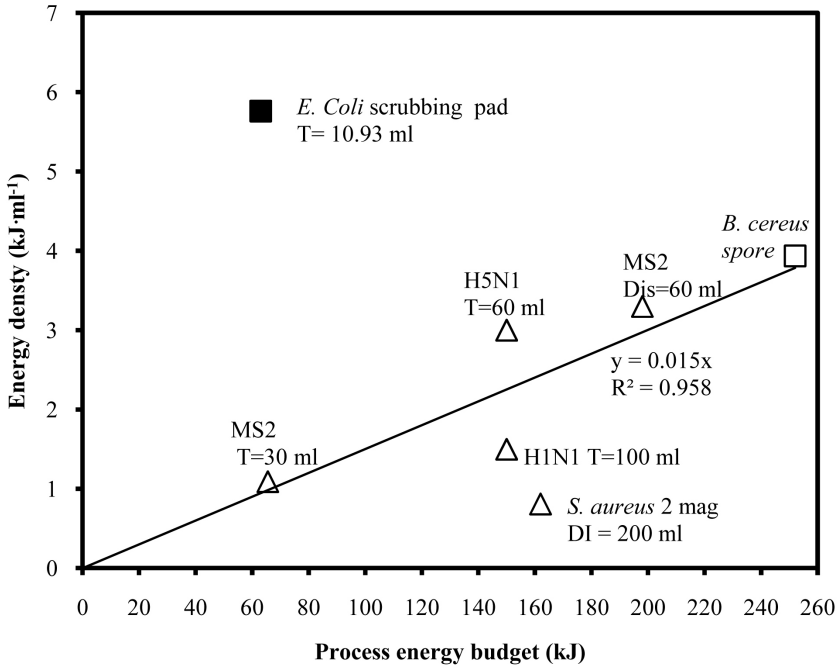

Figure 4. Energy phase-space projection of MGS decontamination dataset (open triangles) overlaid on ≥4 $\log_{10}$ bacteria inactivation for the combined open beaker and kitchen soaked sponge with suspension (solid line). For comparison purposes only, the *E. coli* contaminated kitchen scrubbing pad (black square) and the *B. cereus* contaminated kitchen sponge (open squares) is shown.

The five MGS decontamination data points present a scattered cluster appearance (one on, 2 above, and 2 below the original trend-line). Their scattered appearance indicates a number of possible independent variables operating within the MGS dataset. Some of the variables are now considered. Firstly, the bacteriophage MS2 and influenza virus data points fall within the 63 to 198 kJ process energy budget with the Gram-positive *S. aureus* at the two thirds 162 kJ mark, indicating a possible higher resilience to microwave stress when compared to than the influenza viruses. Note the *B. cereus* spore contaminated sponge data point (open squares) has a value of 252 kJ, some 90 kJ higher than *S. aureus*. Secondly, the water purity (tap, deionized or distilled) reveals there is no clear difference in the decontamination outcome. However, the amount of water used does generate a clear trajectory across the trend-line (60 ml above and 100 and 200 ml below the trend-line); indicating the trajectory is primarily derived from the specific energy calculation ($kJ{\cdot}m1^{-1}$). Secondly, as regards to whether the mode of water reservoir has a deterministic role in the process, the data indicates the sterilizer reservoir has the greatest variance from the trend-line. It is not clear if this variance is due to the use of two cavity-magnetrons, or due to the gram-positive *S. aureus* resilience to microwave stress.

5.2. Kitchen Sponge, Kitchen Scrubbing Pad, and Cigarette Papers

Microwave-assisted decontamination of porous fomites used for cleaning and

re-use (kitchen sponges, scrubbing pad and towels) differ from decontamination and re-use of cigarette filter and N95-like respirators, in that prior and after irradiation the fomites are normally hand squeezed to remove excess liquid before re-use. Such a physical procedure on cigarette filters and N95-like respirators would destroy their filtering performance and fit [22]-[27]. It is therefore informative to see how varying the degree of contaminated water in a porous fomite appears in the energy phase-place projection, and if predictive information can be gained. In addition syringes that present a hard surface are of interest. Due to their size and internal volume the listed fomites large dynamic range of the energy density values (0.2 to 2520 $kJ \cdot ml^{-1}$), to display and access this (as suggest by the delegates of the 14th international on Chaos, Athens, Greece, June 20202) the inactivation data is now displayed in the log-linear format. **Figure 3** shows such a log-linear energy phase-space projection where the ≥4 $\log_{10}$ inactivation [3] [11] [13] [16] is given. In this projection, four iso-volume linear trend-lines for suspension volumes: 5, 10.93, 64, and 100 ml are also given.

In the case of the kitchen sponge and kitchen scrubbing pad data, two additional data points have been generated (indicated by the direction arrow and open triangles from 10.93 to 5 ml, respectively) to represent the theoretical hand squeezing of the sponge and scrubbing pad specific density values to microwave irradiation. To replicate the face towels experiments, the amount of water within two towels (30 × 30 cm (EU/UK standard) and 30 × 46 cm (similar to the Japanese standard) were experimentally determined. Both were soaked in running tap water, and then wrung tight to leave the towels moist. During this process, the weight of the dry, soaked and moist face towels were recorded, from which the moisture content is computed as shown in **Table 3**. The calculated energy density for these two towels is shown as a blue circle and blue diamond, respectively.

For the HCV and HIV decontaminated experiments [11]: the insulin syringe data point was calculated using a contaminated suspension value of 40 ml, and the HCV and HIV-1 spiked cigarette filter data points (blue square) were calculated using a value of 0.5 ml [59]. Finally, for the Park *et al.* [16] decontamination of empted syringe data points, the dead-space and residual syringe suspension on the syringe internal surfaces is estimated to be in the order of 0.1 ml.

Using the above experimental and calculated knowledge, **Figure 5** is constructed. In this figure it is shown that the majority of vegetative *E. coli* data points are clustered in the low 20 to 100 kJ process budget region. Within this

Table 3. Face towel conditions: dry, soaked, and moist weight: plus computed final moisture content of face towel prior to microwave irradiation.

Face towel	Dry weight Size: weight	Soaked weight	Moist weight	Water content in moist face towel
Half size	30 × 30 cm: 50 g	365 g	152 g	233 ml
Full size	30 × 46 cm: 75 g	500 g	225 g	275 ml

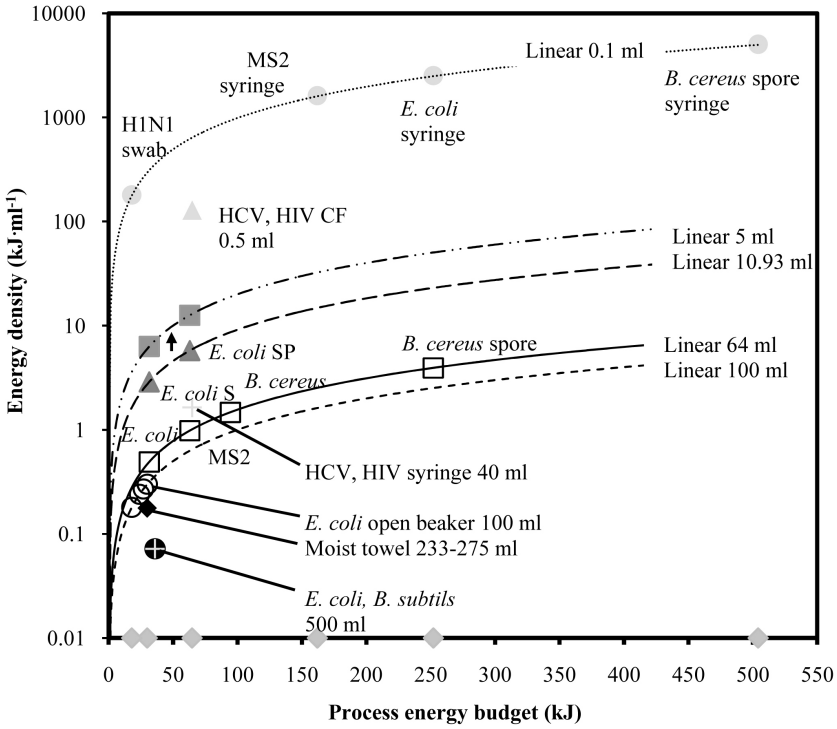

Figure 5. Energy phase-space projection (log-linear) for microwave-assisted ≥ 4 $\log_{10}$ inactivation of microorganism suspensions within different fomites; *E. coli* beaker 100 ml suspension (open circles), *E. coli* kitchen sponge (S: triangle to square), *E. coli* kitchen scrubbing pad (SP: green triangle to green square), moist towel (black diamond). H1N1 swab, MS2 syringe, *E. coli* syringe, and *B. cereus* spore on the 0.1 ml iso-volume trend-line (blue square). Spiked (0.5 ml) cigarette filter (CF: blue triangle).

region the HCV and HIV 40 ml insulin syringe reached a temperature of 56˚C to 60˚C. At the bottom of this cluster, the *E. coli* and *B. subtilis* data points that have recorded SEM and TEM observations of membrane lysis and membrane rupture [14] are present. Above this region, the HCV and HIV spiked (0.5 ml) cigarette filter (70˚C) is located. A little father on, the H1N1 swab (40˚C) and the bacteriophage MS2 contaminated empty syringe (40˚C) form the lower region of the energy budget values for the 0.1 ml iso-volume trend-line. Along this trend-line and with increasing surface syringe temperature *E. coli* (80˚C) and *B. cereus* spore (107˚C to 120˚C) complete the iso-volume trend-line. It is also noted that this series of microorganism have an extended process energy budget values with respect to the microorganism cluster, indicating that the syringe dielectric properties and geometry has a role in the enhancing microorganism resilience to microwave stress. Of further note is that the 64 ml *B. cereus* spore contaminated kitchen sponge (87.2˚C) and the 0.1 ml *B. cereus* spore syringe suspension (107˚C to 120˚C) form energy budget outliers: with the greatest process budget energy of all the data points (252 and 525 kJ, respectively). The kJ disparity between the 0.1 and 64 ml *B. cereus* suspensions reveals that fomite type (dielectric material geometry and suspension volume) alter *B. cereus* spore resilience to microwave stress.

These observations are in-line with microwave power absorption efficiency simulations and measurements for water [59], particularly at small load volumes (<250 ml) [37] when compared to volume of the microwave oven cavities (28 to 45 liters) reported here. In our case we use the units of $kJ \cdot m^{-1}$ to quantify the energy utilization efficiency within the inactivation process, whereas [37] [60] use the relative power absorbed in the load volume to quantify the energy utilization efficiency. Consequently for a syringes of similar dielectric properties, load volumes that have low energy density values achieve lower temperatures for a given process energy budget with respect to loads volumes having high energy density values.

Figure 6 compares the MGS data (open circles) that was originally presented in Figure 1 with separate *E. coli* 64 and 100 ml suspension data points and their respective iso-volume trend-lines have a 0,0 intercept and a $R^2 = 1$. Using this mapping, it is evident that MGS data points cluster around the 64 and 100 ml iso-volume trend-lines. The data demonstrates the difference in resilience to microwave stress for Gram-positive vegetative bacteria (*S. aureus*) and *B. cereus* spore as compared to vegetative Gram-negative *E. coli* bacteria. In the case of microwaved *B. cereus*, SEM imaging reveal disruption of the surface morphology [18]. Also note, again, the MGS MS2 bacteriophage, H1N1 and H2N1 virus data occupy an intimidate microwave stress level between the Gram-negative and Gram-positive bacteria types. This delineation of the MGS dataset into two subsets indicates the resolution and usefulness of the energy phase-space projection.

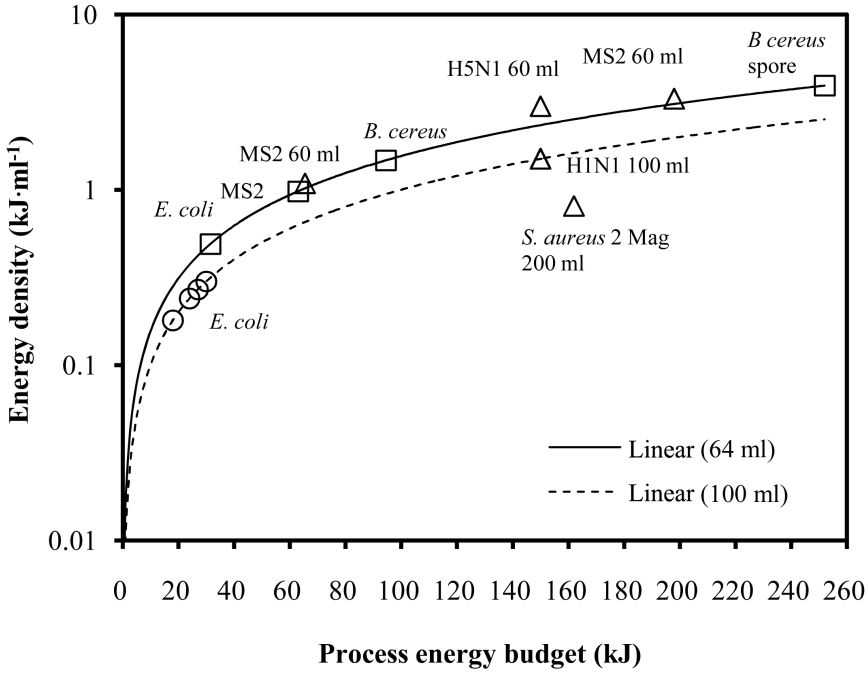

Figure 6. Energy phase-space projection of MGS decontamination datasets (open triangles) overlaid on ≥4 $\log_{10}$ inactivation in 64 ml sponge suspension (open square, solid line) and *E. coli* 100 ml within open beaker (open circle, dashed line).

6. Non-Thermal Microwave-Assisted Inactivation Projection

It is well known that microwave dielectric volumes heating of polar molecules induces the polarization and relaxations of dipoles to generate a rapid temperature rise within dielectric materials, and where temperature rise is rapid compared to thermal heating [35]. The visualization of microorganism resilience to non-thermal microwave-assisted treatment requires the ability to map reversible injury and non-reversible disruption prior to the inactivation state. As microorganism injury and disruption process operate at the top end of environmental temperatures, the inactivation energy phase-state projection has a limited value in this regard. This is because the ice/water dummy-load absorbs a portion of the applied power, plus the extraction of heat from the dielectrically heat suspension vessel. To access the thermal heating data from [31], and non-thermal microwave-assisted treatment [15] [17], the injury and disruption states are mapped using independent variable "process time" on the horizontal-axis and "fomite temperature" on the vertical-axis [30]. Furthermore, as, both "process time" and "fomite temperature" are measured in units of tens, not thousands, a linear scale can be applied. With the limited amount of information regarding heat absorbed by the crystal lattice within ice/water dummy-load given in [15] [17], the approach taken here removes the analysis two heat loss pathways as outliner in Section 2. **Figure 7** shows the data points taken from reference [30], along with the resilience *E. coli* to non-thermal microwave-assisted and thermal heat treatment [15] [17], plus heat inactivation of SARS-CoV strains (urbani, hanoi, and canine) [31].

In this mapping format, the non-thermal microwave-assisted heating of *E. coli* data appear in the bottom left hand corner of the graph with power levels of 200 to 650 W for 40 seconds and suspension temperatures of 20˚C to 29˚C [15] [17]. In this process widow, the *E. coli* suspension controlled to temperature of 20˚C ± 1˚C did not exhibit any change in membrane fluidity or permeabilization [17]. However, the *E. coli* suspensions that were controlled to a temperature of 26˚C to 29˚C [15] resulted in loss of cell viability count. Optical microscope differential fluorescent staining imaging of the treated suspensions revealed that the *E. coli* membrane took on an increasing disrupted appearance with time, without any change in cell shape. Tsuchido *et al.* 1985 [61] reported 55˚C thermal heat disruptive appearance of *E. coli* that may be due to the lost of outer membrane lipopolysacchaides molecules and hence a lost the hydrophilic surface. Rougier *et al.* 2014 [6] has also hypothesized that low levels of pulse discharge induce membrane pore formation and a substantial increase in cellular permeability, where the effect may be temporary or permanent depending on the exposure time.

In contrast to non-thermal microwave-assisted treatment, thermal microwave-assisted ≥4 $\log_{10}$ inactivation is in the 55˚C to 86˚C temperature range and separated into two fomite clusters. The first cluster; open beaker suspension and 40 ml syringe (100 to 650 W), and the second cluster: kitchen sponge, scrubbing

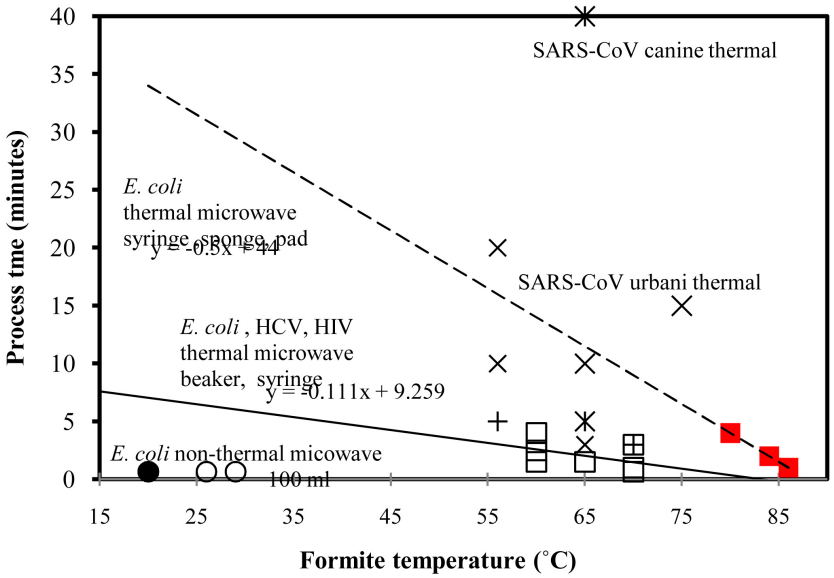

Figure 7. Non-thermal microwave, thermal microwave, and thermal heat treatment of microorganisms plotted as a function of process fomite temperature and process time. The non-thermal and thermal microwave-assisted inactivation is represents as a ≥ 4 $\log_{10}$ reduction. *E. coli* 100 ml suspension; non-thermal microwave (open circles) [15] (black circle) [17]. *E. coli* open beaker thermal microwave (open squares) [12] [14] [17] and HCV and HIV spiked syringe (open cross [11]) combined with dashed trend-line. *E. coli* kitchen soaked sponge and pad, and used syringe (red squares, dotted trend-line) [16]. Thermal inactivation of SARS-CoV-2 suspension data (open stars with trend-line) is taken from [31].

pad and used syringe (1.05 kW). The 7 data points for the open beaker suspension and spiked 40 ml syringe has a dotted trend-line of −0.1113 and temperature intercept of 84˚C. Whereas second cluster (the kitchen sponge, scouring pad, and used syringe) has a dashed trend-line of −0.5 and a temperature intercept of 88˚C. The low process time (typically 2 minutes) reveals the inactivation process is rapid for both cluster, however additional 4˚C intercept for the second cluster indicates the enhanced persistence imparted by kitchen sponge and scouring pad and used syringe.

For comparison purposes, eight thermal ≥ 4 $\log_{10}$ inactivated SARS-CoV stains (urbani, Hanoi and canine) are also plotted in the range of 56˚C to 75˚C. In general the inactivation times are greater than the microwave-assisted treatment, with the SARS canine strain being particularly persistent.

7. Conclusions

This paper has described the use of log-linear energy phase-space projection to analyze multimode microwave oven microwave-assisted ≥ 4 $\log_{10}$ inactivation of bacteria and virus under different fomite conditions. Porous fomites (moist face towels, cotton swabs, kitchen sponges and scrubbing pads, cigarette filters and N95-like respirators), along with hard surface syringe fomites are studied. All of these fomites are classified as dielectric and absorb microwave energy to varying

degrees depending on their complex dielectric properties. Microorganism resilience to microwave stress data is mapped in energy phase-space projection using iso-volume trend-lines, revealing imparted resilience by the fomite. It is also shown that microorganism resilience can be mapped between different microwave ovens. Microorganism resilience imparted by the fomite is shown to increase from vegetative Gram-negative to vegetative Gram-positive and on to Gram-positive spores. Bacteriophage MS2 and influenza viruses have an intermediate resilience dependency. The use of linear-scaled fomite temperature against process time provides a mapping space for differentiating between non-thermal and thermal microwave-assisted treatments. This mapping procedure allows historical microwave-assisted inactivation data to be compared and inform future experiments and microwave-assisted inactivation programs.

The paper has also highlighted five areas where non-thermal (or, athermal) and thermal microwave-assisted treatment of fomite-microorganism system may be further progressed.

1) The ice/water dummy-load used in non-thermal microwave-assisted treatment is complex and still present challenges in the understanding of how energy is absorbed and transported away by the fomite-microorganism system. Furthermore, non-thermal microwave-assisted microorganism injury and disruption experiments require further experimental measurement, and simulation.

2) The deconstruction of historical non-thermal microwave assisted ice/water experiments followed by their re-engineering to map both energy budget and energy density in energy phase-state projection may be possible, with sufficient resolution, to differentiate between *E. coli* and *B. subtilis* that have a similar resilience to microwave stress.

3) Data mining of historical data to extract information relating to the inactivation process may enable burred information within the datasets to be the discovered.

4) Moving from 2-diemenstionl to 3-dimensinal space mapping has a possibility to enhance the visualization of the energy pathway associated with injury, disruption and inactivation processes.

5) The development of mapping tools for aerosol and metal scalpel blades may also extend the understanding of microwave-assisted processing of medical instruments.

Conflicts of Interest

The authors declare they have no conflicts of interest.

References

[1] Metcalf, J.S. and Codd, G.A. (2000) Microwave Oven and Boiling Waterbath Extraction of Hepatotoxins from Cyanobacterial Cells. *FEMS Microbiology Letters*, **184**, 241-246. https://doi.org/10.1111/j.1574-6968.2000.tb09021.x

[2] Orsini, M. and Romano-Spica, V. (2001) A Microwave-Based Method for Nucleic Acid Isolation from Environmental Samples. *Letters in Applied Microbiology*, **33**,

17-20. https://doi.org/10.1046/j.1472-765X.2001.00938.x

[3] Elhafi, G., Naylor, C.J., Savage, C.E. and Jones, R.C. (2004) Microwave or Autoclave Treatments Destroy the Infectivity of Infectious Bronchitis Virus and Avian Pneumovirus but Allow Detection by Reverse Transcriptase-Polymerase Chain Reaction. *Avian Pathology*, **33**, 303-306. https://doi.org/10.1080/0307945042000205874

[4] de la Hoz, A., Díaz-Ortiz, A. and Moreno, A. (2007) Review on Non-Thermal Effects of Microwave Irradiation in Organic Synthesis. *Journal of Microwave Power & Electromagnetic Energy*, **41**, 45-66. https://doi.org/10.1080/08327823.2006.11688549

[5] Law, V.J. and Denis, D.P. (2018) Domestic Microwave Oven and Fixed Geometry Waveguide Applicator Processing of Organic Compounds and Biomaterials: A Review. *Global Journal of Researches in Engineering*: *A Mechanical and Mechanics Engineering*, **18**.

[6] Rougier, C., Prorot, A., Chazal, P., Leveque, P. and Lepratb, P. (2014) Thermal and Nonthermal Effects of Discontinuous Microwave Exposure (2.45 Gigahertz) on the Cell Membrane of *Escherichia coli*. *Applied and Environmental Microbiology*, **80**, 4832-4841. https://doi.org/10.1128/AEM.00789-14

[7] Pillet, F., Formosa-Dague, C., Baaziz, H., Dague, E. and Rols, M.-P. (2016) Cell Wall as a Target for Bacteria Inactivation by Pulsed Electric Fields. *Scientific Reports*, **6**, Article No. 19778. https://doi.org/10.1038/srep19778

[8] Shaw, P., Kumar, N., Mumtaz, S., Lim, J.S., Jang, J.H., Kim, D., Sahu, B.D., Bogaerts, A. and Choi, E.H. (2021) Evaluation of Non-Thermal Effect of Microwave Radiation and Its Mode of Action in Bacterial Cell Inactivation. *Scientific Reports*, **11**, Article No. 14003. https://doi.org/10.1038/s41598-021-93274-w

[9] Samanlioglu, F. and Bilge, A.H. (2016) An Overview of the 2009 A(H1N1) Pandemic in Europe: Efficiency of the Vaccination and Healthcare Strategies. *Journal of Healthcare Engineering*, **2016**, Article ID: 5965836. https://doi.org/10.1155/2016/5965836

[10] Watkins, J. (2020) Preventing a Covid-19 Pandemic. *BMJ*, **28**, Article No. 368. https://doi.org/10.1136/bmj.m810

[11] Siddharta, A., Pfaender, S., Malassa, A., *et al.* (2016) Inactivation of HCV and HIV by Microwave: A Novel Approach for Prevention of Virus Transmission among People Who Inject Drugs. *Scientific Reports*, **6**, Article No. 36619. https://doi.org/10.1038/srep36619

[12] Fujikawa, H., Ushioda, H. and Kudo, Y. (1992) Kinetics of *Escherichia coli* Destruction by Microwave Irradiation. *Applied and Environmental Microbiology*, **58**, 920-924. https://doi.org/10.1128/aem.58.3.920-924.1992

[13] Tanaka, Y., Fujiwara, S., Kataoka, D., Takagaki, T., Takano, S., Honda, S., Katayose, M., Kinosita, Y. and Toyoshima, Y. (1998) Warming and Sterilizing Towels by Microwave Irradiation. *Yonago Acta Medica*, **41**, 83-88.

[14] Woo, I.S., Rhee, I.K. and Park, H.D. (2000) Differential Damage in Bacterial Cells by Microwave Radiation on the Basis of Cell Wall Structure. *Applied and Environmental Microbiology*, **66**, 2243-2247. https://doi.org/10.1128/AEM.66.5.2243-2247.2000

[15] Barnett, C., Huerta-mounoz, U., James, R. and Pauls, G. (2006) The Use of Microwave Radiation in Combination with EDTA as an Outer Membrane Disruption Technique to Preserve Metalloenzyme Activity in *Escherichia coli*. *Journal of Experimental Microbiology and Immunology*, **9**, 1-5.

[16] Park, D.K., Bitton, G. and Melker, R. (2006) Microbial Inactivation by Microwave

Radiation in the Home Environment. *Journal of Environmental Health*, **69**, 17-24.

[17] Asay, B., Tebaykina, Z., Vlasova, A. and Wen, M. (2008) Membrane Composition as a Factor in Susceptibility of *Escherichia coli* c29 to Thermal and Non-Thermal Microwave Radiation. *Journal of Experimental Microbiology and Immunology*, **12**, 7-13.

[18] Cao, J.X., Wang, F., Li, X., *et al.* (2018) The Influence of Microwave Sterilization on the Ultrastructure, Permeability of Cell Membrane and Expression of Proteins of *Bacillus cereus*. *Frontiers in Microbiology*, **9**, Article No. 1870. https://doi.org/10.3389/fmicb.2018.01870

[19] Wu, Y. and Yao, M. (2010) Inactivation of Bacteria and Fungus Aerosols Using Microwave Irradiation. *Journal of Aerosol Science*, **41**, 682-693. https://doi.org/10.1016/j.jaerosci.2010.04.004

[20] Wang, C., Hua, X. and Zhang, Z. (2019) Airborne Disinfection Using Microwave-Based Technology: Energy Efficient and Distinct Inactivation Mechanism Compared with Waterborne Disinfection. *Journal of Aerosol Science*, **137**, Article ID: 105437. https://doi.org/10.1016/j.jaerosci.2019.105437

[21] Wu, Y. and Yao, M. (2014) *In Situ* Airborne Virus Inactivation by Microwave Irradiation. *Chinese Science Bulletin*, **59**, 1438-1445. https://doi.org/10.1007/s11434-014-0171-3

[22] Fisher, E.M., Williams, J. and Shaffer, R.E. (2010) The Effect of Soil Accumulation on Multiple Decontamination Processing of N95 Filtering Facepiece Respirator Coupons Using Physical Methods. *Journal of the International Society for Respiratory Protection*, **27**, 16-26.

[23] Heimbuch, B.K., Wallace, W.H., Kinney, K.R., Lumley, A.E., Wu, C.Y., Wo, M.-H. and Wander, J.D. (2011) A Pandemic Influenza Preparedness Study: Use of Energetic Methods to Decontaminate Filtering Facepiece Respirators Contaminated with H1N1 Aerosols and Droplets. *American Journal of Infection Control*, **39**, e1-e9. https://doi.org/10.1016/j.ajic.2010.07.004

[24] Fisher, E.M., Williams, J.L., Shaffer, R. (2011) Evaluation of Microwave Steam Bags for the Decontamination of Filtering Facepiece Respirators. *PLOS ONE*, **6**, e18585. https://doi.org/10.1371/journal.pone.0018585

[25] Lore, M.B., Heimbuch, B.K., Brown, T.L., Wander, J.D. and Hinrichs, S.H. (2012) Effectiveness of Three Decontamination Treatments against Influenza Virus Applied to Filtering Facepiece Respirators. *Annals of Occupational Hygiene*, **56**, 92-101.

[26] Zulauf, K.E., Green, A.B., Nguyen Ba, A.N., Jagdish, T., Reif, D., Seeley, R., Dale, A., and Kirby, J.E. (2020) Microwave-Generated Steam Decontamination of N95 Respirators Utilizing Universally Accessible Materials. *American Society Microbiology*, **11**, e00997. https://doi.org/10.1128/mBio.00997-20

[27] Pascoe, M.J., Robertson, A., Crayford, A., Durand, E., Steer, J., Castelli, A., Wesgate, R., Evans, S.L., Porch, A. and Maillard, J.-Y. (2020) Dry Heat and Microwave-Generated Steam Protocols for the Rapid Decontamination of Respiratory Personal Protective Equipment in Response to COVID-19-Related Shortages. *Journal of Hospital Infection*, **106**, 10-19. https://doi.org/10.1016/j.jhin.2020.07.008

[28] Law, V.J. and Dowling, D.P. (2021) MGS Decontamination of Respirators: A Thermodynamic Analysis. *Global Journal of Research in Engineering & Computer Sciences*, **1**, 1-17.

[29] Law, V.J. and Dowling, D.P. (2021) MGS Decontamination of Respirators: Dielectric Considerations. *Global Journal of Research in Engineering & Computer Sciences*, **1**, 6-21.

[30] Law, V.J. and Dowling, D.P. (2022) Microwave Detection, Disruption, and Inactivation of Microorganisms. *American Journal Analytical Chemistry*, **13**, 135-161. https://doi.org/10.4236/ajac.2022.134010

[31] Abraham, J.P., Plourde, B.D. and Cheng, L. (2020) Using Heat to Kill SARS-CoV-2. *Reviews in Medical Virology*, **30**, e2115.

[32] Carpenter, S., Walker, B., Anderies, J.M. and Abel, N. (2001) From Metaphor to Measurement: Resilience of What to What. *Ecosystems*, **4**, 765-781. https://doi.org/10.1007/s10021-001-0045-9

[33] Cumming, G.S. and Collier, J. (2005) Change and Identity in Complex Systems. *Ecology and Society*, **10**, Article No. 29. https://doi.org/10.5751/ES-01252-100129

[34] Looyenga, H. (1965) Dielectric Constants of Heterogeneous Mixtures. *Physica*, **31**, 401-406. https://doi.org/10.1016/0031-8914(65)90045-5

[35] Rosapina, S., Salvatorelli, G. and Anzanel, D. (1994) The Bacterial Effect of Microwaves on Mycobacterium Bovis Dried on Scalpel Blades. *Journal of Hospital Infections*, **26**, 45-50. https://doi.org/10.1016/0195-6701(94)90078-7

[36] Sun, J., Wang, W. and Yue, Q. (2016) Review on Microwave-Matter Interaction Fundamentals and Efficient Microwave-Associated Heating Strategies. *Materials*, **9**, Article 231. https://doi.org/10.3390/ma9040231

[37] Houšová, J. and Hoke, K. (2002) Microwave Heating—The Influence of Oven and Load Parameters on the Power Absorbed in the Heated Load. *Czech Journal of Food Sciences*, **20**, 117-124. https://doi.org/10.17221/3521-CJFS

[38] European Standard (2011) Industrial Microwave Heating Installations. Test Methods for the Determination of Power Output. CSN EN 61307 ed. 3.

[39] Law, V.J. and Dowling, D.P. (2019) Chap. 14. Microwave Oven Plasma Reactor Moding and Its Detection. In: 12*th Chaotic Modeling and Simulation International Conference*, Springer, Cham, 157-179. https://doi.org/10.1007/978-3-030-39515-5_14

[40] Lee, G.L., Law, M.C. and Lee, V.C.C. (2020) Numerical Modelling of Liquid Heating and Boiling Phenomena under Microwave Irradiation Using OpenFOAM. *International Journal of Heat and Mass Transfer*, **148**, Article ID: 119096. https://doi.org/10.1016/j.ijheatmasstransfer.2019.119096

[41] Hayes, B.L. (2004) Recent Advances in Microwave-Assisted Synthesis. *Aldrichimica Acta*, **73**, 66-71.

[42] Hayes, B.L. and Collins, M.J. (2005) Reaction and Temperature Control for High Power Microwave-Assisted Chemistry Techniques. United States Patent US 6,917,023.

[43] Yap, T.F., Liu, Z., Shveda, R.A. and Preston, D.J. (2020) A Predictive Model of the Temperature-Dependent Inactivation of Coronaviruses. *Applied Physics Letters*, **117**, Article ID: 060601. https://doi.org/10.1063/5.0020782

[44] Zimmermann, U., Pilwat, G. and Riemann, F. (1974) Dielectric Breakdown of Cell Membranes. *Biophysical Journal*, **14**, 881-899. https://doi.org/10.1016/S0006-3495(74)85956-4

[45] Perreux, L. and Loupy, A. (2001) A Tentative Rationalization of Microwave Effects in Organic Synthesis According to Reaction Medium and Mechanism Considerations. *Tetrahedron*, **57**, 9199-9223. https://doi.org/10.1016/S0040-4020(01)00905-X

[46] Law, V.J. and Dowling, D.P. (2021) Chap. 35. Application of Microwave Oven Plasma Reactors for the Formation of Carbon-Based Nanomaterials. In: Skiadas, C. and Diomtiakis, Y., Eds., 13*th Chaotic Modeling and Simulation International Conference*, Springer, Berlin, 467-486.

[47] Costerton, J.W., Ingram, J.M. and Cheng, A.J. (1974) Structure and Function of the Cell Envelope of Gram-Negative Bacteria. *Bacteriological Reviews*, **38**, 87-110. https://doi.org/10.1128/br.38.1.87-110.1974

[48] Augestad, E.H., Bukh, J. and Prentoe, J. (2021) Hepatitis C Virus Envelope Protein Dynamics and the Link to Hypervariable Region 1. *Current Opinion in Virology*, **50**, 69-75. https://doi.org/10.1016/j.coviro.2021.07.006

[49] Schoeman, D. and Fielding, B.C. (2019) Coronavirus Envelope Protein: Current Knowledge. *Virology Journal*, **16**, 69. https://doi.org/10.1186/s12985-019-1182-0

[50] Bruinsma, R.F., Wuite, G.J.L. and Roos, W.H. (2021) Physics of Viral Dynamics. *Nature Reviews Physics*, **3**, 76-91. https://doi.org/10.1038/s42254-020-00267-1

[51] Wood, J.M. (2015) Bacterial Responses to Osmotic Challenges. *Journal of General Physiology*, **145**, 381-388. https://doi.org/10.1085/jgp.201411296

[52] Auer, G.K. and Weibel, D.B. (2017) Bacterial Cell Mechanics. *Biochemistry*, **56**, 3710-3724. https://doi.org/10.1021/acs.biochem.7b00346

[53] Fraser, D. (1951) Bursting Bacteria by Release of Gas Pressure. *Nature*, **167**, 33-34. https://doi.org/10.1038/167033b0

[54] Foster, J.W., Cowan, R.M. and Maag, T.A. (1962) Rupture of Bacteria by Explosive Decompression. *Journal of Bacteriology*, **83**, 330-334. https://doi.org/10.1128/jb.83.2.330-334.1962

[55] Kampf, G., Todt, D., Pfaender, S. and Steinmann, E. (2020) Persistence of Coronaviruses on Inanimate Surfaces and Their Inactivation with Biocidal Agents. *Journal of Hospital Infection*, **104**, 246-251. https://doi.org/10.1016/j.jhin.2020.01.022

[56] Zasada, A.A., Zacharczu, K., Woźnica, K., Główka, M., Ziółkowski, R. and Malinowska, E. (2020) The Influence of a Swab Type on the Results of Point-of-Care Tests. *AMB Express*, **10**, Article No. 46. https://doi.org/10.1186/s13568-020-00978-9

[57] Wahi, A. (2009) Scouring Pad. US. Patent. 2009/0106920 A1. (Issued Apr 30).

[58] Cambruzzi, M. and Macfarlane, P. (2021) Variation in Syringes and Needles Dead Space Compared to the International Organization for Standardization Standard 7886-1: 2018. *Veterinary Anaesthesia and Analgesi*a, **48**, 532-536. https://doi.org/10.1016/j.vaa.2021.01.008

[59] Register, K.M. (2000) Underwater Naturalist. *Bulletin of the American Littoral Society*, **25**, 23-29.

[60] Su, T., Zhang, W., Zhang, Z., Wang, X. and Zhang, S. (2022) Energy Utilization and Heating Uniformity of Multiple Specimens Heated in a Domestic Microwave Oven. *Food and Bioproducts Processing*, **132**, 35-51. https://doi.org/10.1016/j.fbp.2021.12.008

[61] Tsuchido, T., Katsui, N., Takeuchi, A., Takano, M. and Shibasaki, I. (1985) Destruction of the Outer Membrane Permeability Barrier of *Escherichia coli* by Heat Treatment. *Applied and Environmental Microbiology*, **5**, 298-303. https://doi.org/10.1128/aem.50.2.298-303.1985